



Landslides in Mila town (northeast Algeria): causes and consequences

Nadira Bounemeur¹ · Riad Benzaid¹ · Hassiba Kherrouba¹ · Souad Atoub¹

Received: 4 April 2021 / Accepted: 22 March 2022 / Published online: 10 April 2022
© Saudi Society for Geosciences 2022

Abstract

The Mila town (east Algeria) has suffered frequent landslides during the last few decades because of its geological, geomorphological, and seismotectonic setting, as well as the anthropic activities. This research work deals with the landslide susceptibility assessment using frequency ratio (*FR*) and information value (*IV*) methods in GIS technology in this area. Firstly, a landslide inventory map was constructed from interpretation of high-resolution satellite images, field investigations, and bibliographies. Seven various causal factors are lithology, slope, aspect, altitude, land use, INDV, and density of streams. A thematic layer map is generated for every factor using geographic information system (GIS), the lithological units extracted from the geological database of the Mila region. The slope gradient, aspect, and density from streams were calculated from the digital elevation model (DEM). Contemporary land use map and INDV was derived from satellite images and field study. The analysis of the relationship between landslide factors and landslide events was performed in a GIS environment. Consequently, landslide susceptibility maps (LSMs) were produced through the process of classifying the global landslide sensitivity index (LSS) into five classes. Finally, for model verification, the LSMs obtained with the *FR* and *IV* models were confirmed comparing LSMs with the landslide inventory map using both the receiver operating characteristics (ROC) and the seed cell area index (*SCAI*) models. The area under curve (AUC) results demonstrate that the *IV* method has more performance (85.9%) for landslide susceptibility maps (LSMs) than *FR* method (83%). Moreover, the results of the validation using *SCAI* also confirmed that model *IV* was more precise than the *FR* model. The models employed in this study are capable to resolve the issue of the landslide susceptibility of the study area. The obtained susceptibility maps can be used for future land use planning and can be considered as a powerful tool to resolve the spatial distribution of the risk associated to landslides.

Keywords Mila town · Landslide · Causes · Consequences · Landslide susceptibility mapping

Introduction

In northern Algeria, landslides represent alarming geological phenomena because of the economic consequences and human life's losses they cause, principally in urban areas. Hence, they present a serious threat for human lives and their properties and constitute a major constraint for either the economic development or the urban planning of many

cities (Achour et al. 2017, 2018; Benzaid and Tekkouk 2017; Bounemeur et al. 2019). They constitute a major threat to the population, buildings, and various infrastructures in most mountainous regions (Bounemeur et al. 2019; Kherrouba et al. 2019). Mila town experiences many landslides affecting urban areas, including the road network.

The impact of these land instabilities is significantly worsened by the rapid and the uncontrolled development of the urbanization in landslide prone areas, the heavy and prolonged rainfall trend, and the lack and/or inadequacy of initiative to understand landslide hazards and risks (Bourenane et al. 2015, Bourenane et al. 2021; Hadji et al. 2017). Landslides often occur in the rainy seasons particularly during torrential rainstorms recorded between December and February. Each type of earthquake-induced landslide occurs in a particular suite of geologic environments. The work of Keefer (1984) has shown that this “intensity” depends on

Responsible Editor: Zeynal Abiddin Erguler

This paper was selected from the 3rd Conference of the Arabian Journal of Geosciences (CAJG), Tunisia 2020

✉ Nadira Bounemeur
bounemeur_nadira@yahoo.fr

¹ Geological Engineering Laboratory (LGG), Mohammed Seddik Benyahia University, Jijel, Algeria

the magnitude of the earthquake considered: the greater the magnitude of the earthquake, the greater the “intensity” of the ground movements it can trigger. This phenomenon is known throughout northern Algeria: Tellian Atlas domain, where the rainfall regime is concentrated in a short period with heavy and prolonged rainfalls (Bourenane et al. 2015, Bourenane et al. 2021). This study concerns the ground instabilities observed in Mila town.

Nowadays, these landslides constitute a serious threat to local populations and the environment, forming also a constant constraint to urban planning and development, indeed, the rapid, unplanned urbanization, the bad land-use planning, the environmental mismanagement, and a scarcity of risk mitigation strategy exacerbate the impact of hazards and increase the risk. Unfortunately, there was insufficient consideration of the landslide phenomena in the local strategy of development and land use planning of the town. Indeed, very little research is available on the prediction and prevention of these events, despite the continuous progression of landslides and their associated damage effects (Djerbal et al. 2014; Bourenane et al. 2021). In order to scale back the damage to properties and therefore the losses of human lives also on contribute to the risk reduction for the sustainable urban planning and development of the Mila town, it becomes necessary to generate comprehensive landslide susceptibility maps (LSMs); the landslide susceptibility mapping is considered as an imperative task that can help authorities to reduce landslide disaster losses by serving as a guideline for durable land-use planning such as the restriction of urban extension in hazardous zones. According to Varnes (1984), landslide susceptibility is defined as the probability of the spatial occurrence of landslides in a given area for a given predisposing terrain factors. The landslide susceptibility mapping is related to the subdivision of a given area into homogeneous zones and their ranking according to their degrees of landslide susceptibility; thus, an LSM indicates areas likely to be affected by landslides in the future based on the correlation with historical distributions of landslides and their associated factors. In Algeria, despite the increase and spread of landslides occurrences, there are nevertheless limited and insufficient initiatives in landslide susceptibility mapping. Nevertheless, there are examples of successively performed studies (Bourenane et al. 2015, Bourenane et al. 2021; Djerbal et al. 2014, 2017; Achour et al. 2017; Hadji et al. 2017; Zighmi et al. 2019; Merghadia et al. 2020).

In this study, simple method was went to landslide susceptibility mapping, by following three essential steps: the primary one consists of gather the info input, the other, calculated the landslide susceptibility index using two models supported GIS. Step three, establishment and validation of

the output data. These methods are tested and validated; the results are compared and discussed. This research work may be a part of a thematic approach focused on the understanding of the landslide hazard and also on a strategy of evaluation and mapping of landslide hazard at an outsized scale. Thus, this investigation completes the different works undertaken on the prediction of landslides in urban areas in order to improve the scientific understanding and the spatial variation of landslide hazard in Mila town. The final results provide valuable orientations for landslide hazard reduction and may serve as guidelines for land use development planning in Mila town.

The aim of this study is to provide and develop a deterministic-statistical approach for landslide susceptibility assessment by applying two different methods. The first is an analytic frequency ratio process which a multi-parametric method that was originally developed by Lee and Talib (2005). The second one is a statistical approach based on information value that was proposed by Yin and Yan (1988) and modified slightly by Van Westen (1993). These models were tested, and the results were discussed. The obtained susceptibility map of landslides constitute a basic document for all layout proposed in the future.

Study area

Mila region is located in the northeast of Algeria, about 391 km from Algiers and 50 km northwest of the city of Constantine. It belongs to the Mila basin, which covers an area of 3500 km² often known as the Mila-Constantine basin. Located between latitude 244,591.01 and 263,859.46 m N and longitude 4,027,529.17, 4,043,981.06 m E (WGS 84 UTM 32) (Fig. 1), where the area of this municipality is 129.95 km². The study site named El Kherba is located south of the town of Mila, at an average altitude of 620 m, on slope terrain with an average angle of 14° dipping toward the north (Tebbouche et al. 2022) where the landslide object of our study is located. From a geomorphological point of view, the area of El Kherba is characterized by the presence of plains, mountains, and plateaus; the altitude range varies between 0 and 1099 m on the reliefs (Fig. 1).

Hydroclimatological characteristics of the site

The Mila region is characterized by a Mediterranean climate that is cold and rainy in winter, hot and dry in summer, and receives a height of precipitation varying between 500 and 600 mm/year. The study of climatic data from the ANRH (1993) of Constantine also shows that the rainiest month of the year is the month of December to February, with an average rainfall which oscillates around 39.49%. Slope instability increases considerably during this period,

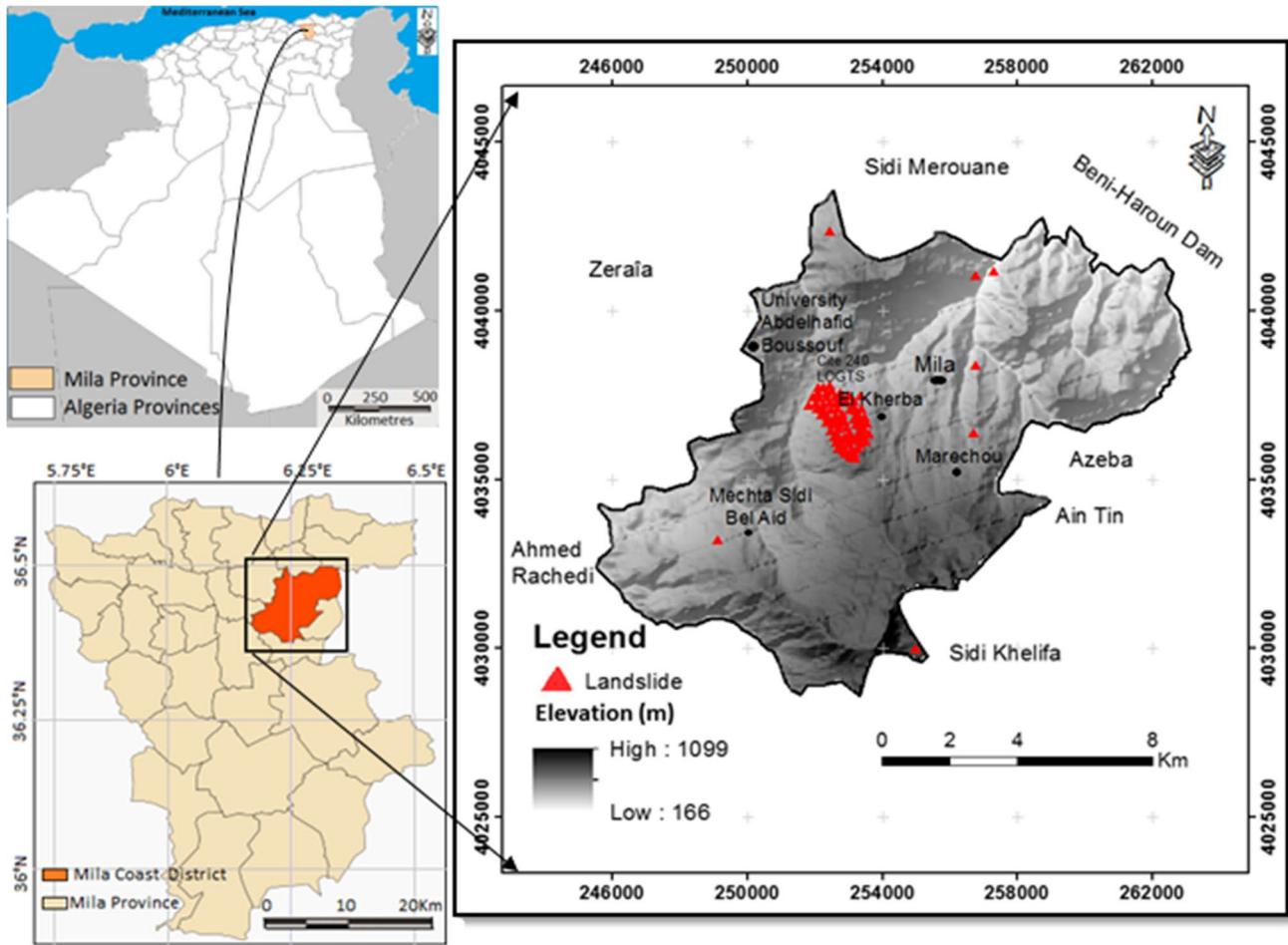


Fig. 1 Location map of the study area, showing the topographic relief

the driest month being July, with an average rainfall of around 6.30% of annual precipitation. Without forgetting the hydrographic network which is very dense in the Mila region and plays a destructive role causing sometimes considerable damage to the various infrastructures of the city, and it is thus that, for the future of the cities, the hydrological elements have a major impact on their physiognomy and on the urban development and the acceleration of the erosive processes of gully, undermining of the banks, and the transport of solid materials. The wadi's region is as follows: Mila Wadi separates the old town from the colonial village, El Kherba Wadi separates the subdivision Boulmerka from the university site, Makraoued, and el Bordjia Wadi (Fig. 2). So the density and organization of the hydrographic network accentuate all the forms of instability of the slopes, landslides and differential erosion very apparent throughout these flows. The role of natural vegetation and human actions cannot be overlooked.

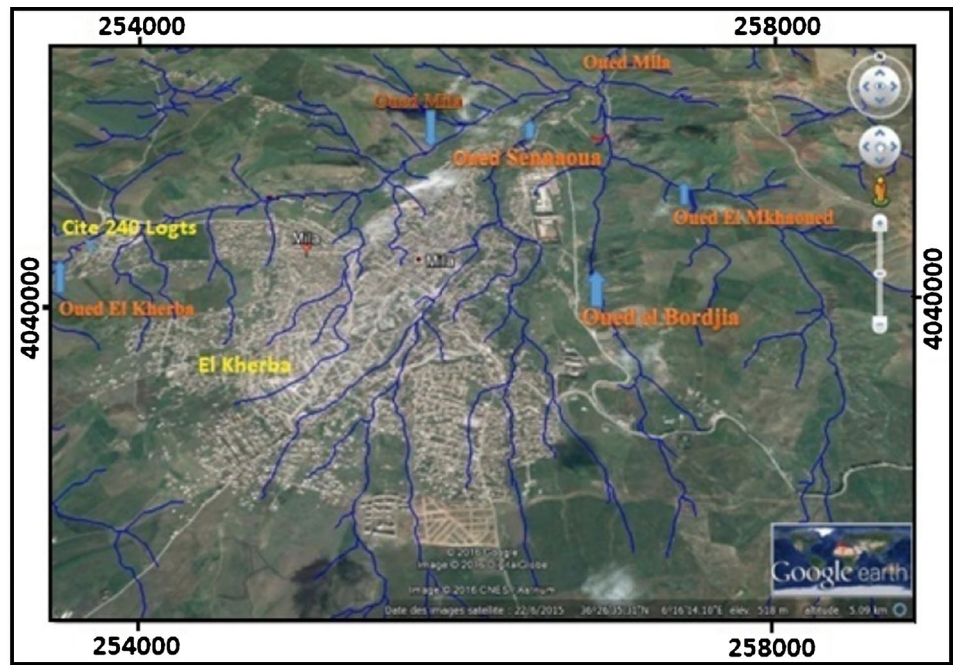
Thematic data preparation

In the present susceptibility analysis, database includes an inventory map in the study area and a set of landslide predisposing factors.

Landslide inventory map

Landslide inventory mapping is one of the key processes for modeling landslide susceptibility (Fell et al. 2008; Corominas et al. 2014; Thiery et al. 2007). Satellite images, GPS, articles, internal reports... and field surveys provide important tools for establishing a landslide inventory map. This map contains a landslide position that occurs in the past. In this study, landslide positions were identified using existing database, satellite images, aerial photos, Google Earth, and terrain

Fig. 2 Hydrographic network in Mila region



studies. Finally, the database contains more than 80 polygons. Figure 1 illustrates the spatial distribution of the landslides' location in Mila town. In this study, we are used the classification of landslides developed by Cruden and Varnes (1996). Landslides are grouped into three types: rotational, translational, and any. Figure 3 illustrates the flowchart of the methodology used in this

research, and Fig. 4 illustrates examples of landslides affecting the study area.

In this work, one approach is use for the mapping of the susceptibility to landslides (Fig. 3); quantitative approach based on weighting criteria (informative value method IV) in a GIS environment. The results could constitute a timely guideline for land use planning in the Mila region (Bourenane et al. 2016; Corominas et al. 2014).

Fig. 3 Methodology flowchart for the process work

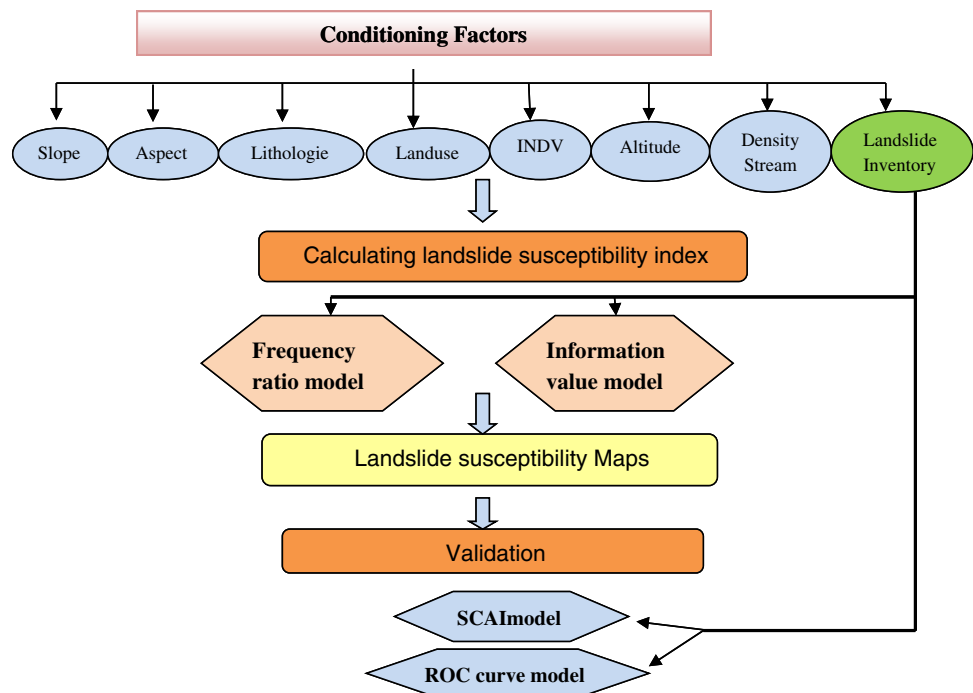


Fig. 4 Examples of the most recent landslides occurred in 2020 that caused ground deformations and severe damage to buildings, roadways, and public infrastructures in the urban area of Mila city (Bounemour 2019)



Landslide conditioning factors

The conditioning factors used in this research are as follows.

Lithology

Lithology, through variations in its structure and properties, is one of the most important factors influencing the occurrence of landslides (Ayalew and Yamagishi 2005), as different lithological units are characterized by different degrees' susceptibility (Dai and Lee 2001; Yalcin and Bulut 2007; Nefeslioglu et al. 2008). A detailed analysis of the lithological characteristics was carried out for the study area on the basis of the main lithological units described in the map geological data available, supplemented by field surveys (Ficheur 1899; Vila 1977; Coiffait et al. 1977; Coiffait 1992; Bougdal et al. 2006). The Mila region is characterized by seven lithological classes (Fig. 5a), while the lithological nature of the studied site shows a predominance of silty clays and/or marls to a depth of about 10 m. The analysis of the observations made on the ground showed that the majority of landslides are mainly recorded in these clayey-marly formations or Mio-Pliocene formation seriously threatens all infrastructures, dwellings, and the road network.

Slope gradient

Slope is a measure of the rate of change in elevation in the direction of the steepest descent and is generally taken into

account for the dynamics of the processes governing the development of terrain. Slope is the main cause of landslides. Because of this direct relationship between slope angle and landslides, it is frequently used to prepare landslide susceptibility maps. The slope gradient map of the study area is shown in Fig. 5b. We note that the highest density of landslides is in the (20–30°) class, followed by the (10–20°) category.

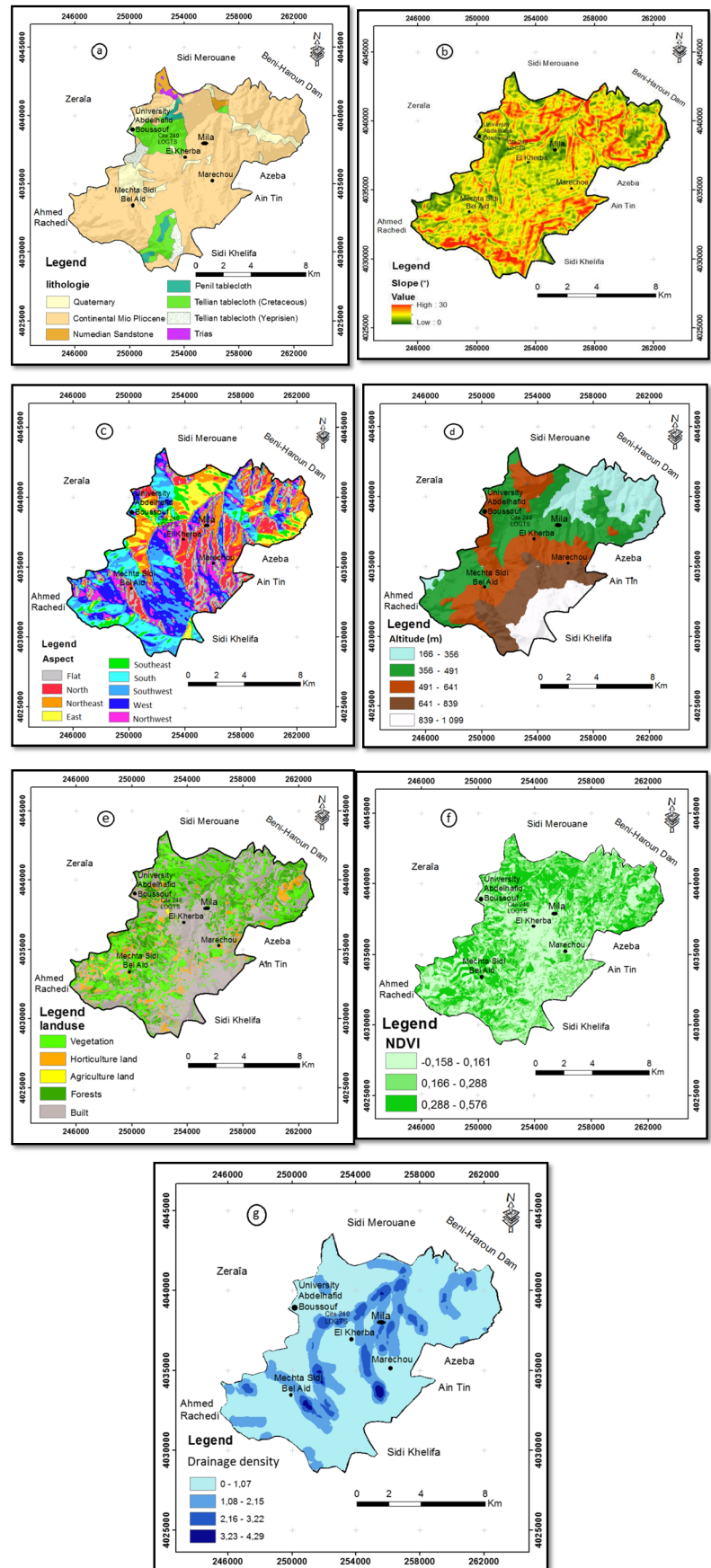
Slope aspect

The aspect is defined as the direction of the compass in which a point is measured in degrees from north in a clockwise direction, ranging from 0 to 360°. Slope exposure is considered to be an important factor indirectly influencing slope stability, as the effect of climatic conditions (such as sunlight, winds, precipitation, and snow) controls humidity and water content of the soil and therefore these mechanical characteristics, which determine the risk of landslides (Magliulo et al. 2008; Dieu et al. 2011; Bourenane et al. 2015). The map (Fig. 5c) is showing that the slopes of Mila town have been classified into nine classes. The slopes oriented from north to south dominate the study area.

Altitude

The intensity of slope movements increases with elevation; in this study, digital elevation model (DEM) was used to perform an elevation map based on the reclassification

Fig. 5 **a** Lithology; **b** slope; **c** appearance; **d** altitude; **e** use of land; **f** NDVI; **g** density of wad (datum reference: WGS 84, UTM zone 32)



function in ArcGIS. The altitudes have been classified into five classes, ranging between 166 and 1099 m (Fig. 5d).

Land use

Arid and poorly vegetative lands make the slope more prone to erosion and landslide (Gomes et al. 2005), so land use considered as an important parameter included in this study. Production of a land use map of Mila town by digitizing a land use map using google explore, it is reclassified into five classes: vegetation, horticulture land, agriculture land, forests, and built and empty land (Fig. 5e).

Normalized difference vegetation index

Vegetation significantly influences the stability of natural slopes (Bo et al. 2008). The normalized difference vegetation index, also called NDVI, is constructed from red (R) and near infrared (PIR). The normalized vegetation index highlights the difference between the visible band of red and that of the near infrared. $NDVI = (PIR - R)/(PIR + R)$ (Fig. 5f).

Drainage density

The study area is characterized by a dense hydrographic network (Fig. 5g). This hydrographic network is a factor

which plays an important and direct role in the triggering of ground instabilities (Gostelow, 1991) and may have an influence on the distribution of unstable areas (landslides) by modifying the behavior of the ground by erosion of the ravines which can initiate the rupture of the slopes. Different studies, such as those of Dai and Lee (2001, 2002), have highlighted the influence of density and the organization of the hydrographic network accentuates all forms of instability of slopes, landslides, and differential erosion clearly visible throughout these flows.

The earthquake effect

In last years, the Mila region has experienced by several earthquakes, which have generated significant material losses and damage to buildings and infrastructure. CRAAG (n.d.) said a tremor was detected on Friday, July 17, 2020, at 9:12 a.m. of magnitude 4.5 degrees on the Richter scale. The same source specifies that the epicenter of this shock was located 1 km north of Sidi Merouane (Mila province). The second earthquake of magnitude 4.9 on the Richter scale, which occurred on Friday morning 08/07/2020 in the same region (Fig. 6), strongly impacted many homes. This earthquake, whose epicenter was located 2 km southeast of Hammala, in the same province, caused a giant crack for several kilometers, crossing fields and places of residence. Fortunately, no human loss has been reported. According to the first images taken by

Fig. 6 Damage observed by landslide caused by earthquake in Mila region



citizens but also by civil protection teams dispatched to the site, hundreds of houses were severely impacted. In other words, the cracks were such that they are no longer habitable. The earthquake caused the complete collapse of two houses in the old town of Mila and a 4-story building in the district of El Kherba. The total area of El Kherba affected by the earthquake is 220 hectares.

Landslide susceptibility analysis

Landslide susceptibility mapping and analysis is done using frequency ratio and information value methods.

Frequency ratio model

The fundamental concept of this method is to calculate the ratio between the density of phenomena in a given class and the density of the same class (Lee and Talib 2005). *LSI* expressed using (Eq. 1):

$$FR = \frac{\text{Landslide pixel class}}{\text{Area pixel class}} = \frac{\% \text{Landslide pixel class}}{\% \text{Area pixel class}} \quad (1)$$

In the study area, the frequency ratio (*FR*) for each causative factor class was calculated using Eq. 1.

After calculating the *FR* for every landslide conditioner factor using Microsoft Excel under ArcGIS, the *FR* value for every factor class was assigned by the joint within the ArcGIS tool. Subsequently, the landslide weighting factors were rasterized using the spatial analysis search tool. Afterward, the landslide susceptibility index (*LSI*) is estimated by summation the frequency ratio of every factor type or class by the Map Algebra raster calculator of the spatial analysis tool and using (Eq. 2):

$$LSI_{FR} = FR * Slope + FR * Aspect + FR * INDV + FR * landuse + FR * lithology + FR * Altitude + FR * DensityStream \quad (2)$$

where *LSI* is the landslide susceptibility index, and *FR* is the frequency ratio of each landslide factor class. After the calculation of *LSI*, the index values were ranked and classified into different landslide susceptibility levels, in order to establish the final LSM using the standard deviation method in ArcGIS tool. The mean value of *FR* is equal to 1. If the value is > 1 , indicates a maximum correlation and a lower value than 1 presents minimal correlation. Table 1 shows the results of this application.

Information value model

The statistical method used in this study is proposed by Yin and Yan (1988) and modified by Van Westen (1993),

is based on the comparison between the spatial distribution of phenomena and their various factors. First, the method is based on a statistical analysis using (Eq. 3):

$$Wi = \ln \left(\frac{\text{Conditional probability } CP}{\text{Prior probability } Pp} \right) = \ln \frac{Densclass}{Densmap} = \ln \frac{Npix(Si)/Npix(Ni)}{\sum_{i=1}^n Npix(Si) / \sum_{i=1}^n Npix(Ni)} \quad (3)$$

where *Wi* is the weight given to the class of a particular thematic layer (e.g., clay or limestone in the layer lithology), *Densclass* is the landslide density within the thematic class, *Densmap*, is the landslide density within the entire thematic layer, *Npix(Si)* is the number of landslide pixels in a certain thematic class, *Npix(Ni)* is the total number of pixels in a certain thematic class, and *n* the number of classes in a thematic map. The natural logarithm is used to accommodate the large variation in the weights; the weight map of the causal factors considered can be overlaid and integrated in GIS software. The total weight (*Wi*) of each thematic layer in study area are determined and reported in Table 1. Finally, the weighted layers resulting were summed up (Eq. 4) (Van Westen 1997):

$$LSI = Wi_{slope} + Wi_{Aspect} + Wi_{INDV} + Wi_{Landuse} + Wi_{Lithology} + Wi_{Altitude} + Wi_{DensityStream} \quad (4)$$

Results and discussion

Seven causative factors (Fig. 5) related to the causes of landslide occurrence including slope, aspect, altitude, lithology, land use, NDVI, and drainage density have been identified and analyzed, and thematic layers have been derived and prepared mainly from the following (Table 1): (i) the available national databases (geological maps, topographic map, DEM, precipitation map); (ii) aerial photographs and satellite image interpretation and Google Earth imagery analyses; and (iii) field geological investigation. The thematic layers generated in GIS software have been re-sampled in a 30 m × 30 m grid size in order to facilitate the easy raster-based computation. In the analysis, the influence of every predisposing factor on the landslide occurrence, the landslide density for every class of every factor was calculated by dividing the landslide occurrence area by the class's area of every factor; for this purpose, all landslide causative factor maps were converted into raster and classified with the same pixel size (30 m × 30 m) in the same projection using Arc toolbox tools under GIS as a spatial analysis tool. Then, the landslide inventory raster map was overlapped with the landslide factor raster class through the combined spatial analysis tool under toolbox to extract

Table 1 Spatial relationship between each factor contributing to a landslide and the landslide using information value model

Parameters	Classes	Class pixels	% class pixels	Landslide pixels	% landslide pixels	FR	Information value (Wi)
Slope (°)	0–3	9916	6.926	101	3.916	0.010	−0.247
	3–7°	53,301	37.229	1295	50.213	0.024	0.129
	7–15°	72,133	50.383	1133	43.931	0.015	−0.059
	15–25°	7563	5.282	49	1.899	0.006	−0.444
	> 25°	255	0.178	1	0.038	0.003	−0.662
Aspect	Flat	20,051	14.005	462	17.913	0.023	0.106
	North	15,021	10.491	65	2.520	0.004	−0.619
	Northeast	14,042	9.808	29	1.124	0.002	−0.940
	East	9533	6.658	10	0.387	0.001	−1.234
	Southwest	7803	5.450	22	0.853	0.002	−0.805
	South	11,625	8.119	54	2.093	0.004	−0.588
	Southwest	18,152	12.678	181	7.018	0.009	−0.256
	West	22,437	15.671	578	22.411	0.025	0.155
	Northwest	24,504	17.115	1178	45.676	0.048	0.426
	Altitude	166–356	25,569	28.41	118	4.575	0.004
356–491		47,317	52.574	667	25.862	0.014	−0.103
491–641		35,948	39.942	1497	58.045	0.041	0.367
641–839		22,074	24.526	281	10.895	0.012	−0.147
839–1099		13,410	14.9	16	0.620	0.001	−1.175
Land use	Class 1	38,682	26.791	207	8.026	0.005	−0.523
	Class 2	381	0.263	4	0.155	0.010	−0.230
	Class 3	67,663	46.864	1616	62.659	0.023	0.126
	Class 4	26,971	18.680	528	20.473	0.019	0.039
	Class 5	10,682	7.398	224	8.685	0.020	0.069
INDV	Faible vegetation	48,987	34.001	1472	57.076	0.030	0.224
	Moyenne vegetation	57,668	40.026	906	35.129	0.015	−0.056
	Dense vegetation	37,420	25.972	201	7.793	0.005	−0.522
Lithology	Continental Mio-Pliocene	108,090	74.876	2025	78.518	0.018	0.020
	Quaternary	16,386	11.350	70	2.714	0.004	−0.621
	Tellian tablecloth (Cretaceous)	16,776	11.621	439	17.022	0.026	0.165
	Numedian sandstone	3106	2.151	45	1.744	0.014	−0.090
Density	0–1.08	78,342	55.072	2034	79.329	0.025	0.155
	1.08–2.16	22,686	15.947	284	11.076	0.012	−0.160
	2.16–3.23	28,722	20.190	229	8.931	0.007	−0.356
	3.23–4.29	12,502	8.788	17	0.663	0.001	−1.124

landslide pixels for each landslide class of each factor. Then, the influence of each factor class was determined using equations of frequency ratio (Eq. 1) and statistical index (Eq. 3) methods. Finally, the results are summarized in Table 1. The statistical analysis of density based on the observed relationship between each factor and the spatial distribution of landslides is very useful to reveal the correlation between landslide locations and factors. In this study, the landslide density was applied and combined with a GIS to assess the relationship between the susceptibility and the triggering factors with landslide occurrences.

Regarding the geology, the occurrence of landslides in the region of Mila is closely related to the lithology and the soil property variations. In this study, the lithology was classified into seven classes as shown in (Fig. 5a). The landslide density percentage is highest in two lithological classes, continental Mio-Pliocene and the Tellian tablecloth of the Cretaceous flysch.

In terms of geomorphology, the slope gradient (Fig. 5b), the aspect (Fig. 5c), and the elevation (Fig. 5d) are considered as important controlling factors in slope stability. Landslide density is highest in the (20–30°) category

Fig. 7 **a** Landslide susceptibility map produced using frequency model, **b** distribution pie chart of the landslide susceptibility classes

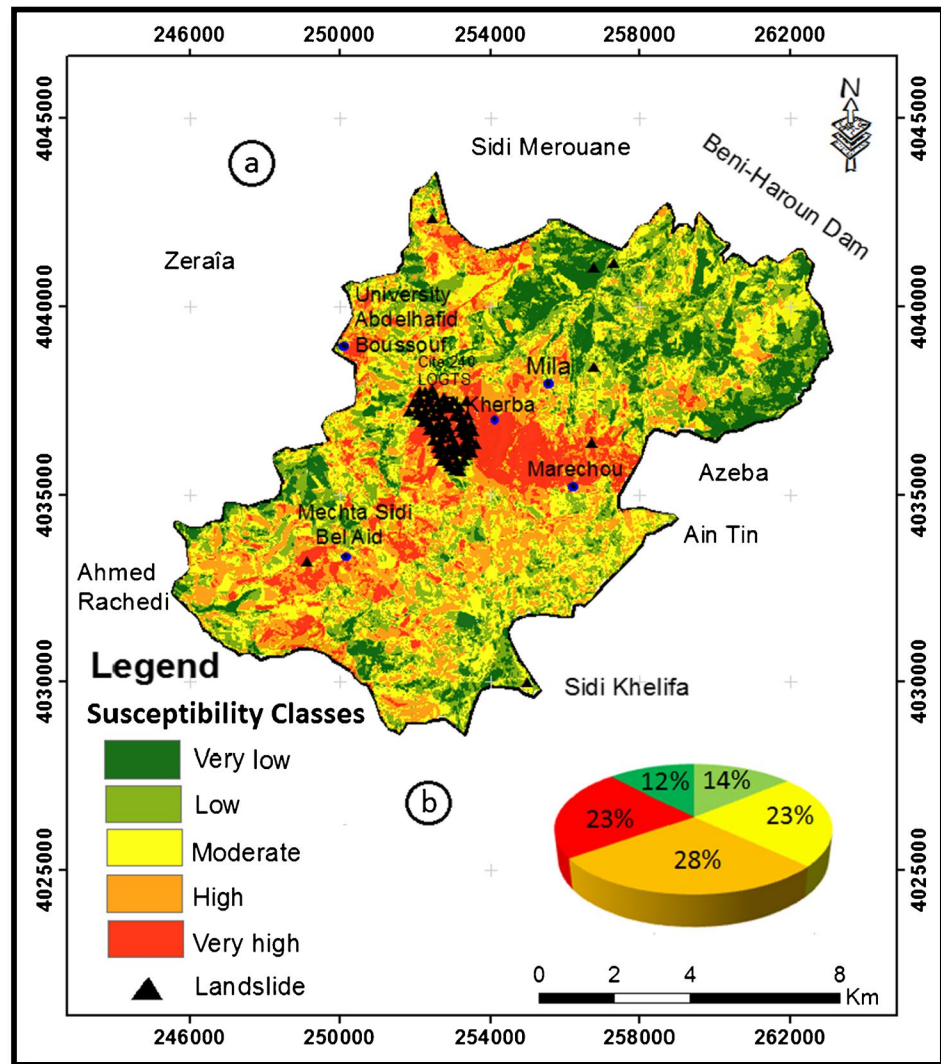


(Fig. 5b). The landslide density percentage is relatively low and increases with the orientation angle (aspect) reaching the maximum at the northwest aspect (Fig. 5c). The northwest oriented slopes are more affected by rainfalls. The elevation is associated with landslides as a result of other factors, the density is highest in the (491–641 m) category, and then decreases (Fig. 5d).

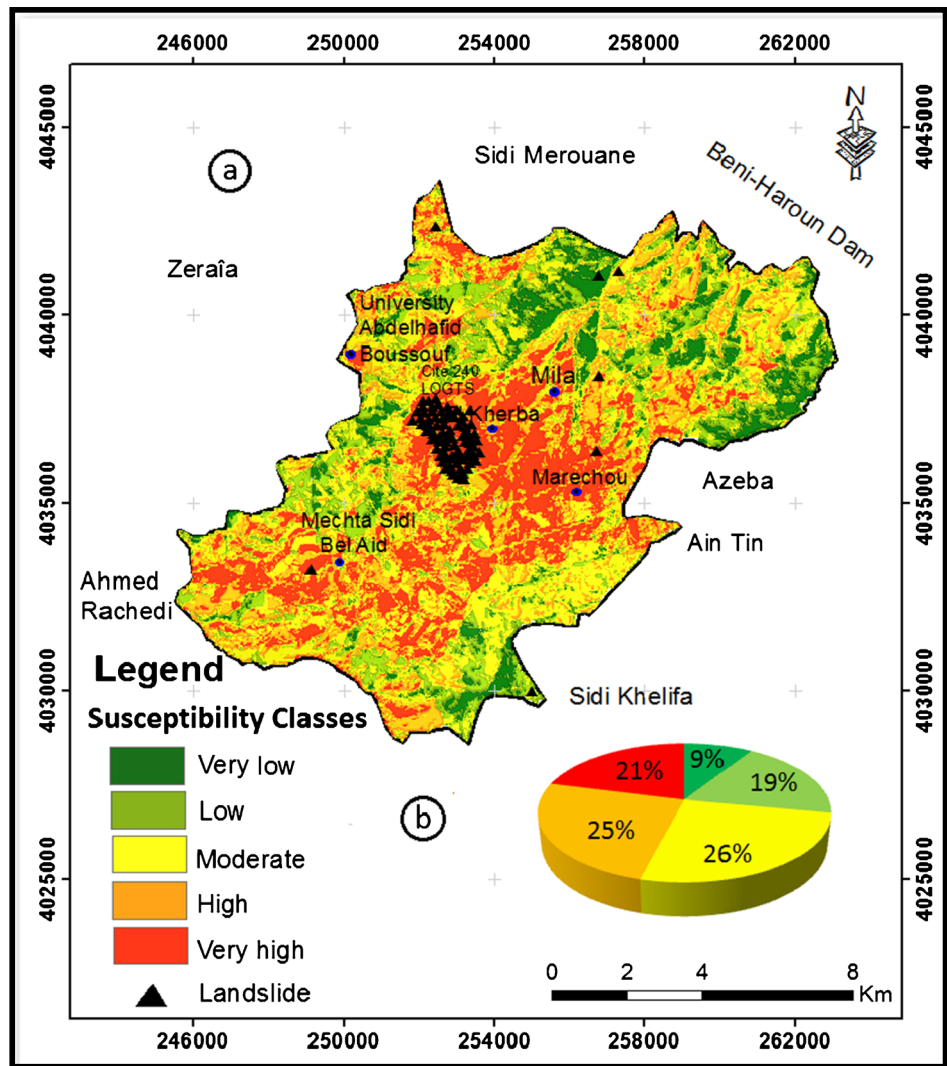
The land use is ranked with the factors causes the landslides in relation especially with the presence/absence of vegetation. In the study area (Fig. 5e), the landslide density is concentrated on the urban area (Fig. 5f). Variation of the vegetation in any area constitutes an important parameter affecting the slope failure, as the slope stability is very sensitive to the changes in vegetation state. The high density of landslides in these areas can be explained by a development of human activity in new inappropriate upland settlements because of the rapid growth of the population.

The distance from main rivers is considered as an important factor in characterizing the landslide susceptible areas. The landslide occurrences increased close to the wadis (Fig. 5g). This generates saturation of the soil and erosion on the banks that activate the dynamics of the slope (slope undercutting and removal of abutment).

Application of frequency ratio

To perform the frequency ratio modeling, every thematic map was crossed with the landslide inventory map using the ArcGIS software, and the *FR* in each class was calculated (Eq. 1). In this analysis, *FR* allowed us to perform a susceptibility model in the study area, showing the importance of each parameter in the occurrence of this event and the relative weight of each parameter class. These weights are presented in Table 1. Consequently, for the degree of slope, *FR* has a maximum value for the slope class (3–7°).

Fig. 8 a Landslide susceptibility map produced using information value model, **b** distribution pie chart of the landslide susceptibility classes



Appearance analyses show that the maximum *FR* value (0.048) is for northwest, followed by west (0.025) and flat (0.023), indicating the maximum probability of landslide occurrence. Parameter lithology frequency results indicate that the gray Tellian tablecloth (Cretaceous) and continental Mio-Pliocene marl with a maximum *FR* value (0.026) is the most prone to landslides.

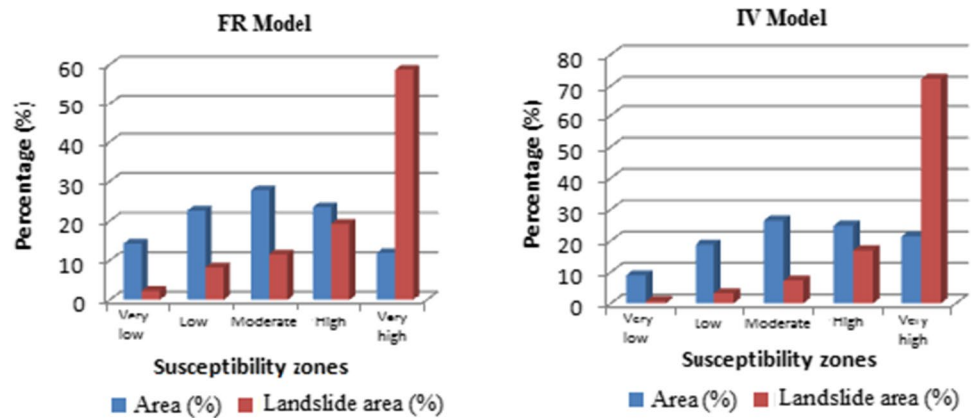
For the density of wadi, *FR* are distributed at a value of 0 to 1.08 indicating a high probability of landslide occurrence. For *FR*, 0.041 corresponds an altitude of 491–641 m. Correlation between land use, vegetation index, and landslides indicates that the landslide occurred respectively in class 3 where NDVI is low corresponds to the increase of *FR* (0.030). Using Eq. 2 and reclassify function, the *LSI* map was reclassified into five classes: very low (14.25%), low (22.61%), moderate (27.75%), high (23.47%), and very high (11.89%) (Fig. 7a, b).

Application of information value

To perform the IV modeling, every thematic map was crossed with the landslide inventory map using the ArcGIS software, and the information value in each class was calculated (Eq. 3). The resultant weights of each thematic map for the IV model are given in Table 1.

The combination thematic maps with the landslide inventory map in ArcGIS calculate the number of landslide pixels in each class. The final calculated *LSI* of the study area for the information value model ranges from 5.059 to 1.596. *LSI*'s positive and negative results mean that higher values indicate a high possibility of slippage. The *LSI* card was classified into five classes using the pauses (jenks) method (very low 8.92%, low 18.67%, moderate 26.34%, high 24.75%, and very high 21.30%) (Fig. 8a, b).

Fig. 9 Histograms showing the distribution of active landslides zones falling into various susceptibility classes of different landslide susceptibility zonation maps



Validation and comparison of the landslide susceptibility maps

For validation of the used models in this study, two statistical methods were used to evaluate the performance of the LSMs obtained. Both of ROC curve and *SCAI* methods are based on the mixture of the landslide susceptibility and landslide inventory map. ROC curve have comparing 30% of the landslide for model validation and 70% of the landslide for training, taking into account their spatial location using the random distribution technique. Then, we have validated the used models using ROC curves (Fig. 9).

The ROC curve is one of the useful statistical strategies used to represent the performance or the exceptional of the landslide susceptibility model. The area under curve (AUC) value is used to evaluate the efficiency of a forecast system by describing the system's ability to predict accurately the non-occurrence or the occurrence of a landslide event (Chung and Fabbri 2003; Yesilnacar and Topal, 2005). The AUC value and the correspondent performance (Yesilnacar and Topal, 2005) can be rated as follows: 0.5–0.6 (poor performance model), 0.6–0.7 (average performance model), 0.7–0.8 (good performance model), 0.8–0.9 (very good performance model), and 0.9–1 (excellent performance model). ROC curves have been obtained by comparing the landslide validation data set, with the two LSMs and the area under curves were calculated for the two landslide models. These results indicate that the

FR model has the highest accurate prediction (83.0%) than the *SI* (85.90%) models (Fig. 10a, b). From there, it is concluded that all the used models in this study showed practically very good accuracy in predicting the landslide susceptibility in the study area. The obtained LSMs had been additionally tested and validated the use of the two statistical regulations for spatial effective LSMs (Bai et al. 2010; Pradhan and Lee 2010). The percentages of landslides within the five susceptibility classes have been determined and presented in Fig. 9. It is deduced that the higher amount of landslides was scattered in the high and very high susceptibility classes, and the smaller amount of landslides was distributed in the low and very low susceptibility classes of the LSMs.

The solution oriented based on the *SCAI* method has been proposed to compare the results of two methods according to the LSM. The *SCAI* method was cited by Süzen and Doyuran (2004) as a validation tool for a landslide susceptibility map. In order to evaluate *SCAI*, we have used the following equation:

$$SCAI = \frac{SAP}{LP}$$

where *SAP* is the area susceptibility percentages and *LP* is the landslide percentage. According to Table 2, very high and high classes contained the minimum *SCAI*, for low and very low classes contain a maximum *SCAI* value. The results of the *SCAI* method confirmed that the *IV* method is more efficient than the *FR* method.

Fig. 10 Receiver operating characteristics (ROC) curve of the LSM. **a** Provide by frequency model, **b** provide by bivariate statistical model

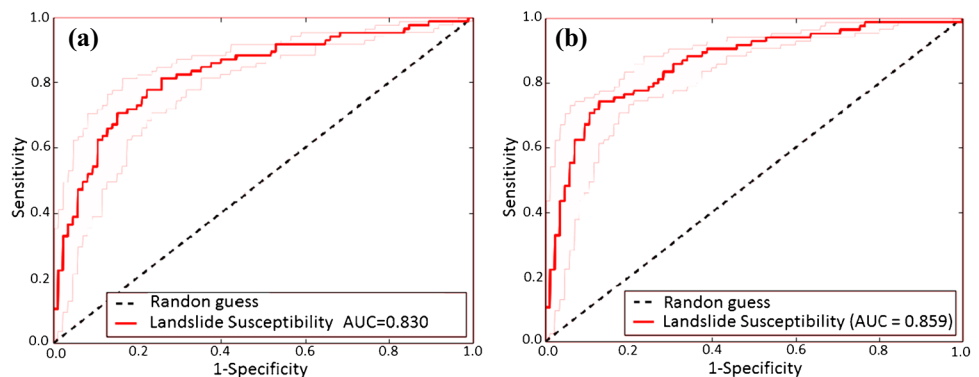


Table 2 Densities of landslide occurrence among the landslide susceptibility classes for the two models

Model Susceptibility classes	FR			IV		
	Area (%)	Landslide area (%)	SCAI	Area (%)	Landslide area (%)	SCAI
Very low	14.25	2.29	6.22	8.92	0.62	14.39
Low	22.61	8.22	2.75	18.67	3.18	5.87
Moderate	27.75	11.55	2.40	26.34	7.21	3.65
High	23.47	19.23	1.22	24.75	16.83	1.47
Very high	11.89	58.70	0.20	21.30	72.16	0.29

Conclusions

Landslides are the most disastrous natural hazards in the northeast of Algeria; their assessment should be done before the construction of all types of engineering projects. In this study, we investigate the potential application of statistical models and the GIS as a relatively new approach for landslide susceptibility mapping in the city of Mila. Firstly, a landslide inventory map was prepared using aerial photographs and satellite image interpretation supported by field surveys. Then, seven landslide predisposing factors including the slope, aspect, altitude, land use, lithology, NDVI, and drainage density have been derived from satellite images, aerial photographs, geological map, DEM, and rainfall database. The LSMs were produced using two methods and classified into five susceptibility classes: low, very low, moderate, high, and very high.

For verification, the LSM obtained was compared to the known location of the landslide using ROC technique. According to the obtained AUC, the IV model has higher prediction performance (85.90%) compared to the FR (83.0%) models. The results revealed also that all the used models provided good accuracy in landslide susceptibility mapping in the Mila town.

The LSMs in this study can be considered as a useful guide for future development and planning of the Mila urban area. These susceptibility maps give information on the spatial prediction probability of landslide in the area; they are a helpful and valuable tool for risk reduction. As our results were given at large-scale mapping, the exact extent of the slope instability areas and details of the high susceptibility areas are well determined; this will be useful for further detailed site-specific studies. The development of urbanization in landslide prone areas can be avoided if the LSM is available. Primarily based on the acquired LSMs, a variety of mitigation strategies has been advocated as a way to lessen the effect of the present landslides which encompass the subsequent: (i) restricting the development planning in landslide-prone areas by using the obtained LSMs; (ii) controlling by means of codes and urban rules the

human activity in the landslide prone areas (i.e., excavation, construction, grading, cutting slopes, landscaping, irrigation activities, vegetation clearance...); (iii) protecting the existing developments by mean of physical mitigation measures (such as drainage, down counterfort berms that serve as buttresses, and protective barriers); finally (iv) developing and implementing of monitoring and warning systems.

Acknowledgements The authors are thankful to the Scientific, Organizing and Technical Committees of the scientific event CAJG 2020. The authors would like to acknowledge the anonymous reviewers for their constructive suggestions. They also want to express their gratitude to everyone who provided assistance in realizing this study.

Declarations

Conflict of interest The authors declare no competing interests.

References

- Achour Y, Boumezbeur A, Hadji R, Chouabbi A, Cavaleiro V, Bendaoud EA (2017) Landslide susceptibility mapping using analytic hierarchy process and information value methods along a highway road section in Constantine, Algeria. Arab J Geosci 10(8):194
- Achour Y, Garçia S, Cavaleiro V (2018) GIS-based spatial prediction of debris flows using logistic regression and frequency ratio models for Zêzere River basin and its surrounding area, Northwest Covilhã, Portugal. Arab J Geosci. <https://doi.org/10.1007/s12517-018-3920-9>
- ANRH (1993) Rainfall map of northern Algeria at 1: 500,000. Explanatory note - National agency for hydraulic resources, Algiers, 49 p
- Ayalew L, Yamagishi H (2005) The application of GIS-based logistic regression for landslide susceptibility mapping in the Kakuda-Yahiko Mountains, Central Japan. Geomorphology 65(1):15–31
- Bai S, Wang J, Lu G, Zhou P, Hou S, Xu S (2010) GIS-based logistic regression for landslide susceptibility mapping of the Zhongxian segment in the Three Gorges area, China. Geomorphology 115:23–31. <https://doi.org/10.1016/j.geomorph.2009.09.025>
- Benzaid R, Tekkouk M (2017) Study of stability of the slope of access to the viaduct of Wadi Dib, Northeast Algeria. Am J Civil Environ Eng 2(3):21–29

- Bo NW, Fabius M, Fabius K (2008) Impact of global warming on stability of natural slopes. Proceedings of the 4th Canadian conference on geohazards: from causes to management. Presse de l'Université Laval, Québec, p 594
- Bougdal R, Belhai D, Antoine P (2006) Geology of the city of Constantine and its surroundings. *Bull Serv Geol Algeria* 18:3–23
- Bounemur N, Benzaid R, Atoub S (2019) Landslides in the Mila basin-AGIS approach. In: Kallel A. et al. (eds) Recent advances in geo-environmental engineering, geomechanics and geotechnics, and geohazards. CAJG 2018. Advances in science, technology & innovation (IEREK interdisciplinary series for sustainable development). Springer, Cham. https://doi.org/10.1007/978-3-030-01665-4_100
- Bourenane H, Meziani A, Ait Benamar D (2021) Application of GIS-based statistical modeling for landslide susceptibility mapping in the city of Azazga, Northern Algeria. *Bull Eng Geol Env* 80:7333–7359. <https://doi.org/10.1007/s10064-021-02386-0>
- Bourenane H, Bouhadad Y, Guettouche MS, Braham M (2015) GIS-based landslide susceptibility zonation using bivariate statistical and expert approaches in the city of Constantine (Northeast Algeria). *Bull Eng Geol Environ* 74:337–355
- Bourenane H, Guettouche MS, Bouhadad Y, Braham M (2016) Landslide hazard mapping in the Constantine city, Northeast Algeria using frequency ratio, weighting factor, logistic regression, weights of evidence, and analytical hierarchy process methods. *Arab J Geosci* 9:1–24
- Chung CJ, Fabbri AG (2003) Validation of spatial prediction models for landslide hazard mapping. *Nat Hazards* 30:451–472. <https://doi.org/10.1023/B:NHAZ.0000007172.62651.2b>
- Coiffait PE, Vila JM, Guellal S (1977) Geological map d'El Aria at 1/50000
- Coiffait Ph-E (1992) Un bassin post-nappes dans son cadre structural: l'exemple du bassin de Constantine (Algerie Nord-Orientale). Thèse DoctoratEs-Sciences, H. Poincaré University, Nancy I, France, 502 p. In French
- Corominas J, Van Westen C, Frattini P, Cascini L, Malet JP, Fotopoulou S, Catani F, Van DenEeckhaut M, Mavrouli O, Agliardi F, Pitolakis K, Winter MG, Pastor M, Ferlisi S, Tofani V, Herva's J, Smith JT (2014) Recommendations for the quantitative analysis of landslide risk. *Bull Eng Geol Env* 73:209–263
- CRAAG (n.d.) Astronomical, Astrophysical and Geophysical Research Center-Algeria
- Cruden DM, Varnes DJ (1996) Landslide types and processes, special report. Transport Res Board, Natl Acad Sci 247:36–75
- Dai FC, Lee CF (2001) Terrain-based mapping of landslide susceptibility using a geographical information system: a case study. *Can Geotech J* 38(5):911–923
- Dai FC, Lee CF (2002) Landslide characteristics and slope instability modeling using GIS, Lantau Island, Hong Kong. *Geomorphology* 42(3):213–228
- Dieu TB, Owe L, Inge L, Oystein D (2011) Landslide susceptibility analysis in the Hoa Binh province of Vietnam using statistical index and logistic regression. *Nat Hazards* 59:1413–1444. <https://doi.org/10.1007/s11069-011-9844-2>
- Djeralb L, Alimrina N, Melbouci B, Bahar R (2014) Mapping and management of landslide risk in the city of Azazga (Algeria). *Landslide science for a safer geoenvironment*. pp 463–468
- Djeralb L, Khoudi I, Alimrina N, Melbouci B, Bahar R (2017) Assessment and mapping of earthquake-induced landslides in Tizirt City, Algeria. *Nat Hazards* 87(3):1859–1879. <https://doi.org/10.1007/s11069-017-2831-5>
- Fell R, Corominas J, Bonnard C, Cascini L, Leroi E, Savage WZ (2008) Guidelines for landslide susceptibility, hazard and risk zoning for land use planning. *Eng Geol* 102:85–98
- Ficheur M (1899) Geological map at 1/50 000 of Constantine
- Gomes A, Gaspar J, Goulart C, Queiroz G (2005) Evaluation of landslide susceptibility of Sete Cidades Volcano (S. Miguel Island, Azores). *Nat Hazards Earth Syst Sci* 5:251–257
- Gostelow P (1991) Rainfall and landslides. In: Almeida-Teixeira M, Fantechi R, Oliveira R, Gomes Coelho A (eds) Prevention and control of landslides and other mass movements. CEC, Brussels, pp 139–161
- Hadji R, Rais K, Gadri L, Chouabi A, Hamed Y (2017) Slope failure characteristics and slope movement susceptibility assessment using GIS in a medium scale: a case study from Ouled Driss and Machroha municipalities, Northeast Algeria. *Arab J Sci Eng* 42:281–300. <https://doi.org/10.1007/s13369-016-2046-1>
- Keefer DK (1984) Landslides caused by earthquakes. *Bull Seismol Soc Am* 95:406–421
- Kherrouba H, Lamara M, Benzaid R (2019) Contribution of electrical tomography to the study of landslides in Texenna region (Northeast Algeria). In: Sundararajan N et al (eds) On significant applications of geophysical methods, Advances in science, technology & innovation. https://doi.org/10.1007/978-3-030-01656-2_11
- Lee S, Talib JA (2005) Probabilistic landslide susceptibility and factor effect analysis. *Environ Geol* 47:982–990
- Magliulo P, Di Lisio A, Russo F, Zelano A (2008) Geomorphology and landslide susceptibility assessment using GIS and bivariate statistics: a case study in southern Italy. *Nat Hazards* 47:411–435. <https://doi.org/10.1007/s11069-008-9230-x>
- Merghadia A, Yunusb AP, Douc Jd, Whiteleye J, ThaiPhamg B, Tien-Buihn B, Avtari R, Boumezbear A (2020) Machine learning methods for landslide susceptibility studies: a comparative overview of algorithm performance. *Earth-Science Rev*. <https://doi.org/10.1016/j.earscirev.2020.103225>
- Nefeslioglu HA, Gokceoglu C, Sonmez H (2008) An assessment on the use of logistic regression and artificial neural networks with different sampling strategies for the preparation of landslide susceptibility maps. *EngGeol* 97:171–191
- Pradhan B, Lee S (2010) Delineation of landslide hazard areas using frequency ratio, logistic regression and artificial neural network model at Penang Island, Malaysia. *Environ Earth Sci* 60:1037–1054. <https://doi.org/10.1007/s12665-009-0245-8>
- Süzen ML, Doyuran V (2004) Data driven bivariate landslide susceptibility assessment using geographical information systems: a method and application to Asarsuyu catchment, Turkey. *Eng Geol* 71(3):303–321
- Tebbouche MY, Ait Benamar D, Hassan HM, Singh AP, Raouf B, Machane D, Meziani Adb, Nemer Z (2022) Characterization of El Kherba landslide triggered by the August 07, 2020, Mw =4.9 Mila earthquake (Algeria) based on post-event field observations and ambient noise analysis <https://doi.org/10.1007/s12665-022-10172-8>
- Thiery Y, Malet JP, Sterlacchini S, Puissant A, Maquaire O (2007) Landslide susceptibility assessment by bivariate methods at large scales: application to a complex mountainous environment. *Geomorphology* 92:38–59. <https://doi.org/10.1016/j.geomorph.2007.02.020>
- Van Westen CJ (1993) Application of geographic information systems to landslide hazard zonation. ITC publication, vol 15. International Institute for Aerospace Survey and Earth Sciences, Enschede, p 245
- Van Westen CJ (1997) Statistical landslide hazard analysis. ILWIS 2.1 for Windows application guide. ITC publication, Enschede, pp 73–84
- Varnes DJ (1984) Landslide Hazard Zonation, a review of principles and practice. IAEG Commission on Landslides. UNESCO, Paris, p 63
- Vila JM (1977) Geological map of Constantine 1/200000

- Yalcin A, Bulut F (2007) Landslide susceptibility mapping using GIS and digital photogrammetric techniques: a case study from Ardesen (NE-Turkey). *Nat Hazards* 41:201–226
- Yesilnacar E, Topal T (2005) Landslide susceptibility mapping: a comparison of logistic regression and neural networks methods in a medium scale study, Hendek region (Turkey). *EngGeol* 79(3–4):251–266. <https://doi.org/10.1016/j.enggeo.2005.02.002>
- Yin K, Yan T (1988) Statistical prediction model for slope instability of metamorphosed rocks. *Proceedings of the 5th international symposium on landslides*. pp 1269–1272
- Zighmi K, Hadji R, Hamed Y (2019) GIS based approaches for the landslide susceptibility prediction in Setif Region (NE Algeria). *Geotech Geol Eng* 37(1):359–374. <https://doi.org/10.1007/s10706-018-0615-7>